ELSEVIER

Journal of Chromatography A, 688 (1994) 231–242

JOURNAL OF
CHROMATOGRAPHY A

Thermal decomposition characterization of explosives by pyrolysis–gas chromatography–mass spectrometry

Jehuda Yinon[a,*], Richard A. Yost[a], Suryanarayana Bulusu[b]

[a]*Department of Chemistry, University of Florida, Gainesville, FL 32611, USA*
[b]*US Army Armament Research, Development and Engineering Center (ARDEC), Picatinny Arsenal, NJ 07806, USA*

First received 30 June 1994; revised manuscript received 29 August 1994

Abstract

Pyrolysis–GC–MS was used to study the thermal decomposition products of a series of explosives, including 1,3,5-trinitro-1,3,5-triazacyclohexane (RDX), 1,3,5,7-tetranitro-1,3,5,7-tetrazacyclooctane (HMX), 2,4,6,N-tetranitro-N-methylaniline (tetryl), monoaminotrinitrobenzene (MATB), diaminotrinitrobenzene (DATB) and triaminotrinitrobenzene (TATB). Pyrolysis products were determined as a function of temperature in the range of 400–1000°C. Decomposition products were found to be in the low-molecular-mass range, resulting mainly from the cleavage of the C–C ring structure in the trinitroaromatic compounds and the C–N ring structure in the nitramines. Decomposition pathways and processes were determined for the various explosives.

1. Introduction

Chemical mechanisms, kinetic parameters and thermodynamic properties are key topics in the understanding of the ignition/combustion process and product distribution of explosives. A structural analysis of the fragments and intermediates resulting from controlled heating of energetic compounds can yield important information relevant to the understanding of the thermal processes. Moreover, the characterization of the individual products resulting from the combustion process can provide important data pertinent to the use of incineration of explosives as a way of disposing of obsolete explosives and ammunition. Identification of these products is important in order to single out those which are toxic, so as to avoid environmental pollution.

Pyrolysis in combination with various analytical techniques has been used to study thermal decomposition of explosives. Pyrolysis–thin layer chromatography (Py–TLC) has been used to study the thermal decomposition of 2,4,6-trinitrotoluene (TNT) [1]; pyrolysis–gas chromatography (Py–GC) has been used to identify smokeless powders and their residues [2] and to investigate the thermal decomposition of 1,3,5-trinitro-1,3,5-triazacyclohexane (RDX) and 1,3,5,7-tetranitro-1,3,5,7-tetrazacyclooctane (HMX) [3]; pyrolysis–atmospheric pressure ionization tandem mass spectrometry (Py–API-MS–MS) has been used to study the thermal decomposition of RDX and HMX [4–6]. Thermal decomposition of RDX and HMX has also been largely studied by mass spectrometry itself [7–10], and more

---

[*] Corresponding author. On sabbatical leave from the Weizmann Institute of Science, Department of Environmental Sciences and Energy Research, Rehovot 76100, Israel. Correspondence should be addressed to the Weizmann Institute of Science.

0021-9673/94/$07.00
SSDI 0021-9673(94)00827-2

recently by simultaneous thermogravimetry and modulated beam mass spectrometry [11–15].

The Py–GC–MS technique provides unique advantages for the identification of the pyrolysate products. It incorporates the gas chromatograph for the separation of the various products and the mass spectrometer as an identification tool.

GC, MS and GC–MS and their applications in the analysis of explosives have been extensively reviewed [16]. Pyrolytic methods and instrumentation [17] and Py–GC and Py–MS techniques [18] have also been described.

In order to determine the thermal decomposition products and contribute to the understanding of the decomposition pathways and processes, a Py–GC–MS study of a series of explosives was undertaken. The explosives studied were RDX (**1**), HMX (**2**), tetryl (**3**), monoaminotrinitrobenzene (MATB, trinitroaniline) (**4**), diaminotrinitrobenzene (DATB) (**5**) and triaminotrinitrobenzene (TATB) (**6**).

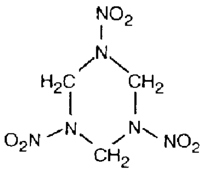

1

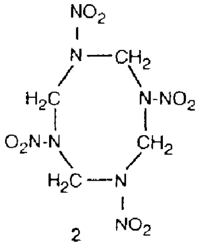

2

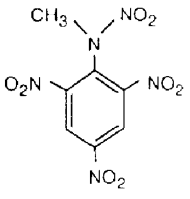

3

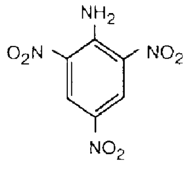

4

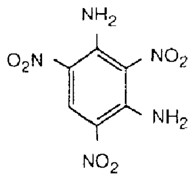

5

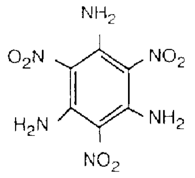

6

2. Experimental

Thermal decomposition of the explosives was carried out with a Pyroprobe 100 solids pyrolyser (Chemical Data Systems, Oxford, PA, USA) equipped with a platinum coil desorption probe. Pyrolysis was carried out with the temperature ramp (rise time) in the off position; the final temperature was set at 400–1000°C and held for 2 s. The sample (approximately 100 μg) was placed in a quartz tube in the form of an acetone solution. After complete drying, the quartz tube was positioned in the platinum coil of the pyrolysis probe. The actual temperatures of the samples in the pyrolysis experiments are uncertain. Therefore, the temperatures set on the pyrolyser should be considered as nominal temperatures. The pyrolyser was interfaced to a Finnigan MAT ITS 40 ion-trap GC–MS system. GC columns used were a 27.5 m × 0.53 mm I.D. PoraPLOT Q fused-silica capillary column with a film thickness of 20 μm (Chrompack, Middelburg, Netherlands) and a 30 m × 0.545 mm I.D. GC-Q porous polymer fused-silica capillary column (J&W Scientific, Folson, CA, USA). A split–splitless injector was used.

Pyrolysis was performed with a flow of helium at a pressure of 20 p.s.i. The flow-rate of helium through the GC column, at 10 p.s.i., was 1 ml/min, which was passed into the ion-trap mass spectrometer. As both GC columns were megabore columns, in order to obtain low flow-rates (necessary for the ion trap), a 0.5-m piece of microbore fused-silica capillary column was connected between the GC column and the ion trap.

The GC conditions were as follows: injector temperature, 175°C; initial column temperature, 35°C (hold time 5 min); heating rate, 15°C/min; final temperature, 200°C (hold time 20 min). The ion trap was operated in the electron impact (EI) mode at a temperature of 220°C and a helium pressure of about $3 \cdot 10^{-4}$ Torr (the gauge reading of the housing pressure was $3 \cdot 10^{-5}$ Torr). Explosive samples were obtained from the US Army Armament Research Development and Engineering Center, Picatinny Arsenal, NJ, USA.

3. Results and discussion

3.1. RDX and HMX

Figs. 1 and 2 show the Py-GC-MS reconstructed ion chromatograms (RIC) (total ion chromatograms) of RDX and HMX, respectively, at 1000°C. One can observe the typical similarity of the two chromatograms.

Fig. 3 shows an example of a mass spectrum of a decomposition product of RDX from pyrolysis at 1000°C. The *m/z* of this product is 70 and is probably due to $C_3H_6N_2^+$. The full list of the molecular ions obtained is given in Table 1.

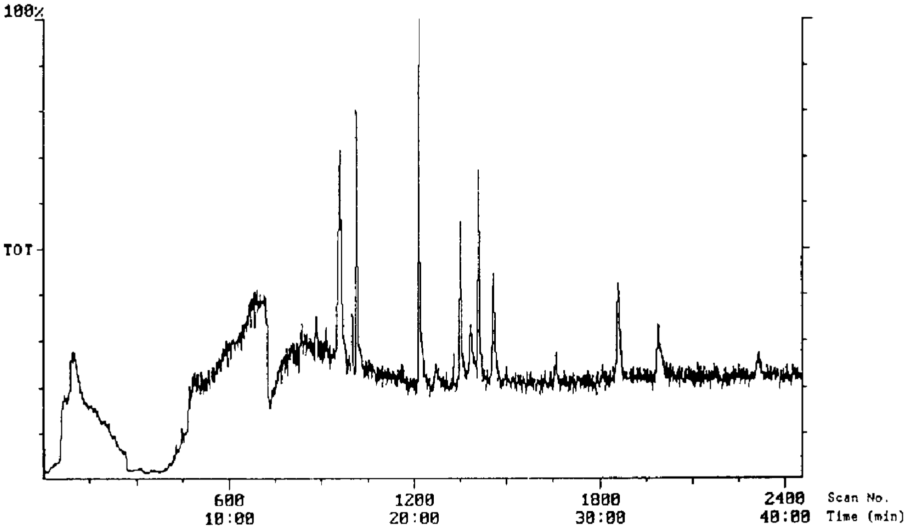

Fig. 1. Py-GC-MS: reconstructed ion chromatogram of RDX at 1000°C.

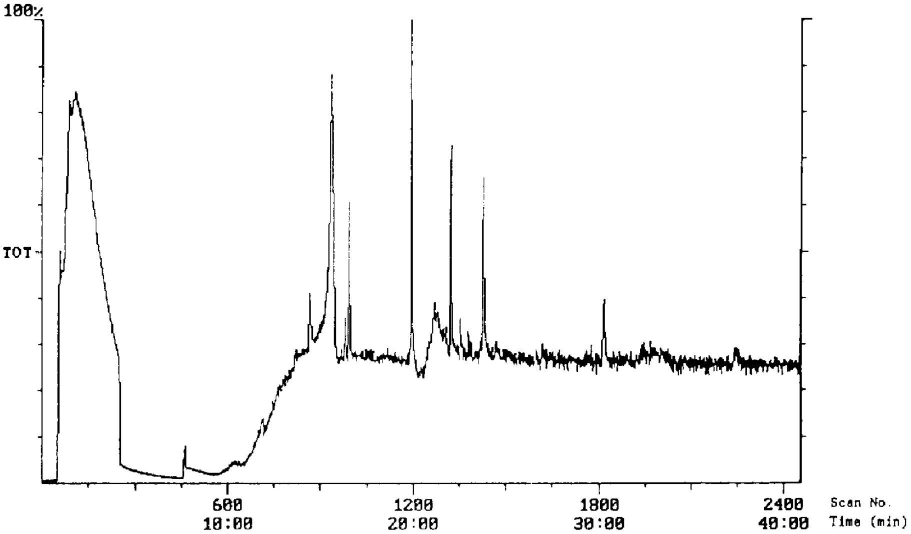

Fig. 2. Py-GC-MS: reconstructed ion chromatogram of HMX at 1000°C.

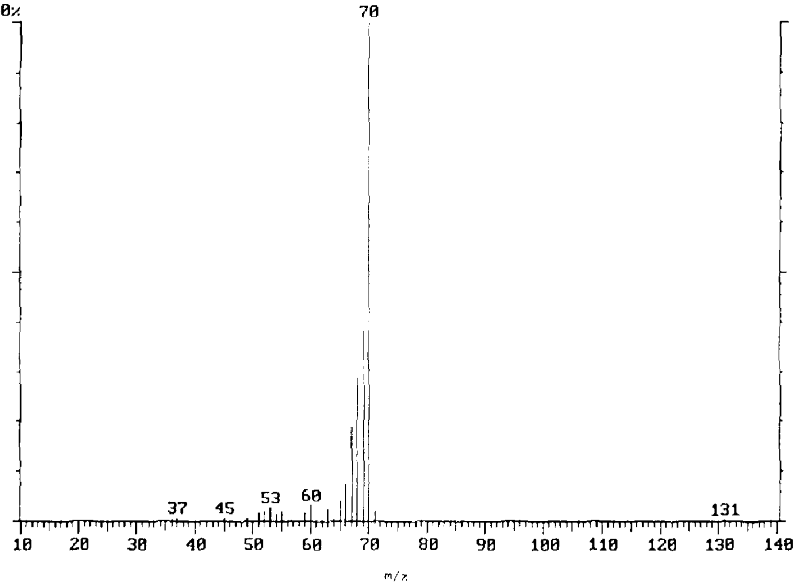

Fig. 3. Py–GC–MS: Py–GC–MS mass spectrum of a decomposition product of RDX from pyrolysis at 1000°C.

Fig. 4 shows an example of a mass spectrum of a decomposition product of HMX from pyrolysis at 1000°C. The *m/z* of this product is 81 and is probably due to $C_3H_3N_3^+$.

As the ion trap is operated at a high pressure of helium, ion–molecule reactions might occur resulting in MH^+ ions. These MH^+ ions should not be confused with the molecular ions. One way to differentiate between them is to look at the mass chromatographic peak shapes. An example is given in Fig. 5, showing the mass chromatograms of *m/z* 74 and 75 ions in the

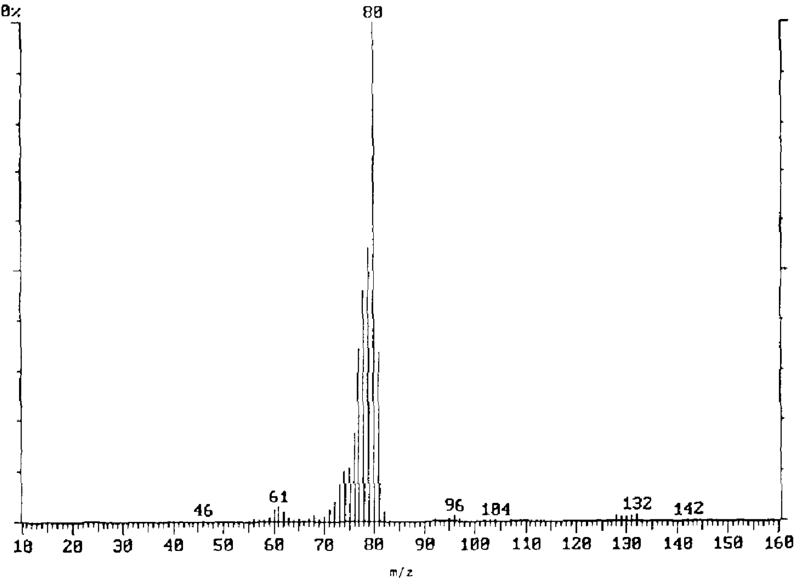

Fig. 4. Py–GC–MS: mass spectrum of a decomposition product of HMX from pyrolysis at 1000°C.

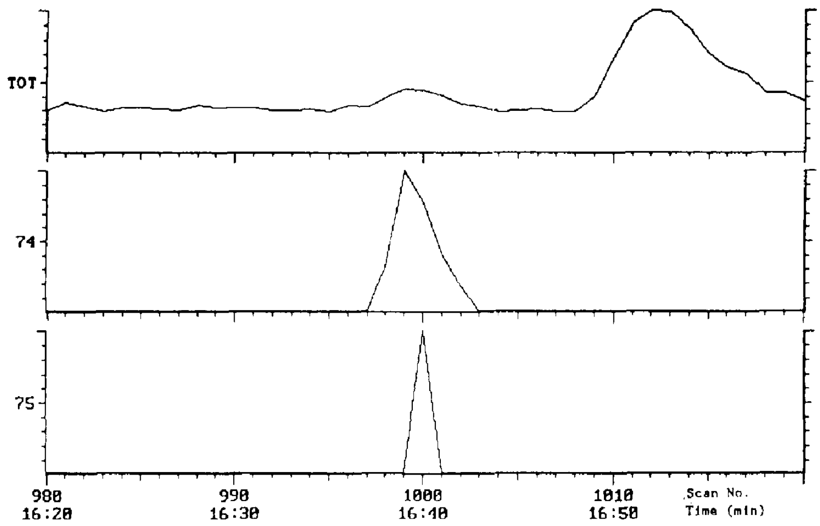

Fig. 5. Mass chromatograms of *m/z* 74 and 75 ions in the Py–GC–MS of RDX.

Py–GC–MS of RDX. The peak of *m/z* 75 is much narrower than that of *m/z* 74, indicating that it is formed through an ion–molecule reaction, when its concentration reached an optimum level.

Table 1 shows the molecular ions obtained in the Py–GC–MS of RDX and HMX and their suggested interpretation. The reproducibility of the pyrograms over an extended period of time was about ±20%. Under these conditions no distinct temperature effect was found in the range 500–1000°C (at 100°C intervals). At 400°C several ions were observed which did not appear at higher temperatures. Table 1 also shows the ions observed in the Py–MS of RDX and HMX by Snyder and co-workers [4,6]. When trying to identify some of the thermal decomposition products, we could only rely on the EI mass spectra and on previously published work [4–6]. The suggested species are shown in Table 2. To obtain positive identification it is necessary to compare the mass spectra with the mass spectra of standards and to carry out MS–MS of both with collision-induced dissociation.

Some of the species listed in Table 1 do not seem to have been observed before, either in pyrolysis studies [4–6] or in thermal decomposition studies [11–15]. Examples are the ions at *m/z* 100, 105 and 106, which probably represent residues containing the original RDX ring. The ion at *m/z* 97 (oxy-*s*-triazine) was previously observed as an important intermediate in the decomposition of RDX [12].

In order to determine the decomposition processes in RDX and HMX, as a first step, mainly the ions observed in both compounds were taken into consideration, as the decomposition processes in both compounds are expected to be similar. The pattern of thermal decomposition will therefore be shown here only for the case of RDX.

The thermal fragmentation pathways of the RDX molecule are depicted in Fig. 6. There is an initial loss of most NO_2 groups as a result of the cleavage of the N–N bond, followed by cleavage of two C–N bonds. Some of these fragments decompose further to produce the lower molecular mass fragments $C_2H_2^+$, CN^+, CH_2N^+, CO^+, NO^+, CH_2O^+, $CHNO^+$ and CH_2NO^+.

It is assumed that the thermal fragmentation pathways of HMX are similar, as most of the ions obtained in the Py–GC–MS of HMX are identical with those of RDX.

Table 1
Molecular ions obtained in the Py–GC–MS of RDX and HMX

m/z	RDX	HMX	Suggested formula	Refs. [4] and [6]		
				RDX	HMX	Formula
26	+	+	$C_2H_2^+$ or CN^+			
28	+	+	CH_2N^+ or CO^+			
30	+	+	NO^+ or CH_2O^+			
43	+[a]	+[a]	$CHNO^+$ or $C_2H_5N^+$		+	C_2H_5N
44	+	+	CH_2NO^+ or $C_2H_6N^+$			
45	–	+[a]	CH_3NO^+	+	+	CH_3NO
53	+	+	$C_3H_3N^+$ or $C_2HN_2^+$			
57	+[a]	–	$C_2H_3NO^+$ or $C_2H_5N_2^+$		+	C_2H_3NO
58	+	+	$C_2H_4NO^+$ or $C_2H_6N_2^+$			
59	+	+	$C_2H_5NO^+$ or $CH_3N_2O^+$	+	+	C_2H_5NO
60	–	+[a]	$CH_4N_2O^+$			
70	+	+	$C_3H_6N_2^+$		+	$C_3H_6N_2$
71	–	+[a]	$C_2H_3N_2O^+$ or $C_3H_5NO^+$			
72	+	–	$C_3H_6NO^+$			
73	+	+	$C_3H_7NO^+$	+	+	C_3H_7NO
74	+[a]	+[a]	$C_2H_6N_2O^+$	+	+	$C_2H_6N_2O$
75	–	+[a]	$CH_3N_2O_2^+$ or $C_2H_7N_2O^+$			
81	+	+	$C_3H_3N_3^+$			
82	+	–	$C_3H_4N_3^+$		+	$C_4H_6N_2$
96	+	–	$C_3H_2N_3O^+$			
97	+	+	$C_3H_3N_3O^+$	+	+	$C_3H_3N_3O$
98	+	–	$C_3H_4N_3O^+$			
99	+	–	$C_3H_5N_3O^+$			
100	–	+	$C_3H_6N_3O^+$ or $C_4H_8N_2O^+$			
105	+[a]	–	$C_2H_5N_2O_3^+$			
106	–	+[a]	$C_2H_6N_2O_3^+$ or $C_2H_8N_3O_2^+$			

+ = Obtained; – = not obtained.
[a] Obtained only at a low temperature of 400°C.

Table 2
Suggested thermal decomposition species in RDX and HMX

m/z of molecular ion	Suggested species	Formula	Also seen in Ref.
43	Ethylenimine	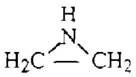	[13]
	N-Methylmethyleneimine	$H_3CN{=}CH_2$	
45	Formamide	$HCONH_2$	
59	Acetamide	CH_3CONH_2	[12]
	Methylformamide	$HCONHCH_3$	
70	–	$CH_2{=}NCH_2N{=}CH_2$	[3]
73	N,N-Dimethylformamide	$HCON(CH_3)_2$	[12,15]
74	N-Nitrosodimethylamine	$(CH_3)_2NNO$	
81	Triazine	$C_3H_3N_3$	

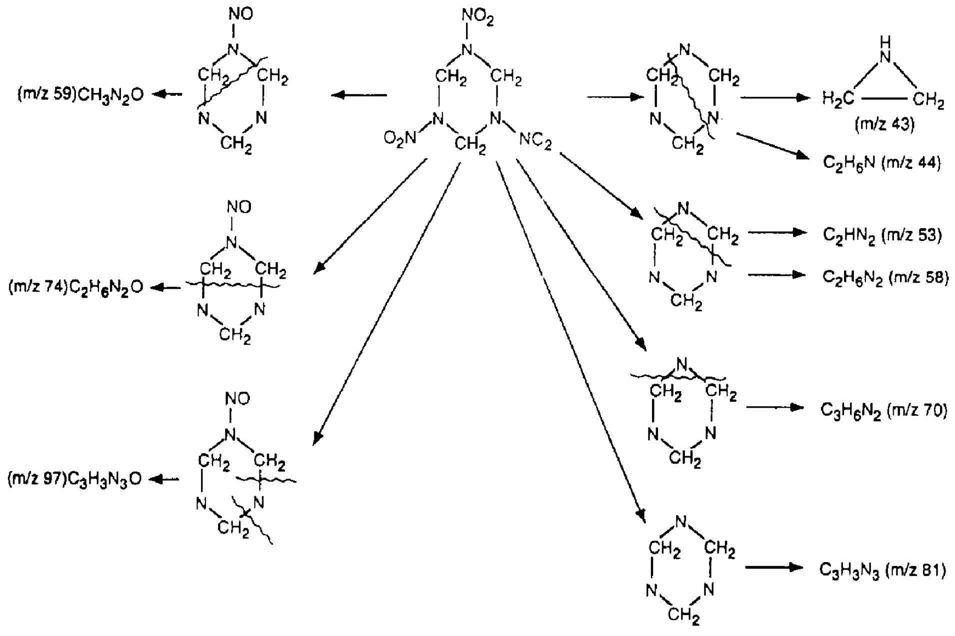

Fig. 6. Thermal fragmentation pathways of RDX.

3.2. *MATB, DATB and TATB*

Fig. 7 shows the Py–GC–MS RIC of MATB at 800°C. Fig. 8 shows an example of a mass spectrum of a decomposition product of MATB from pyrolysis at 800°C. This product is probably due to $C_4H_3N_2^+$.

Table 3 shows the molecular ions obtained in the Py–GC–MS of MAT, DATB and TATB and their suggested interpretation. No major tem-

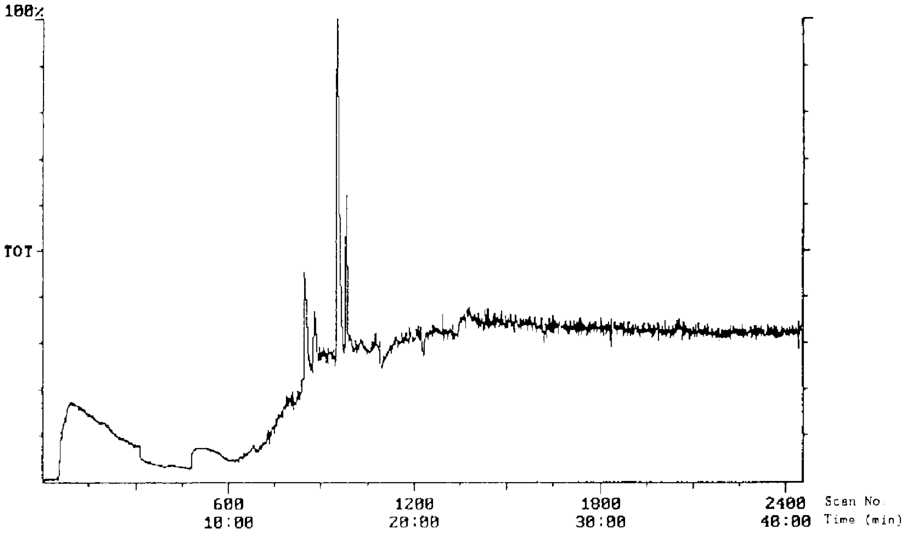

Fig. 7. Py–GC–MS: reconstructed ion chromatogram of MATB at 800°C.

Table 3
Molecular ions obtained in the Py–GC–MS of MATB, DATB and TATB

m/z	MATB	DATB	TATB	Suggested formula
26	+	+	+	CN^+
28	+	+	+	CH_2N^+ or CO^+
30	+	+	+	NO^+
43	−	+	+	$CHNO^+$
44	−	+	+	CH_2NO^+ or CO_2^+
45	+	−	−	CH_3NO^+ or HCO_2^+
51	+	−	−	C_3HN^+
53	+	−	−	$C_2HN_2^+$
54	+	−	−	$C_2H_2N_2^+$
57	−	−	+	$C_2H_3NO^+$
58	+	+	+	$C_2H_4NO^+$ or CNO_2^+
59	−	+	+	$CHNO_2^+$ or $C_2H_5NO^+$
63	−	−	+	$CH_5NO_2^+$
78	−	+	−	$C_4H_2N_2^+$
79	+	−	−	$C_4H_3N_2^+$
82	−	+	−	$C_4H_4NO^+$
87	−	−	+	$C_2H_3N_2O_2^+$
91	+	−	−	$C_5H_3N_2^+$
96	−	−	+	$C_4H_4N_2O^+$
98	+	−	−	$C_3H_2N_2O_2^+$
104	+	−	−	$C_2H_4N_2O_3^+$

+ = Obtained; − = not obtained.

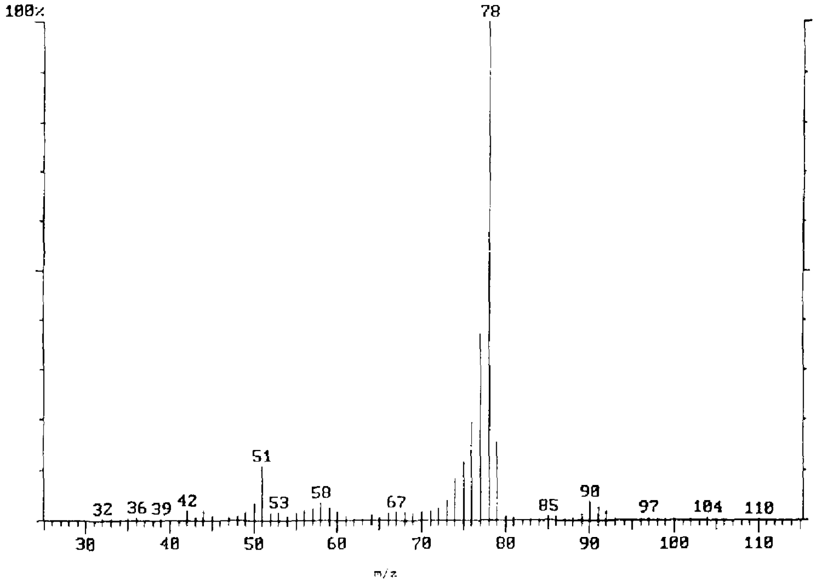

Fig. 8. Py–GC–MS: mass spectrum of a decomposition product of MATB from pyrolysis at 800°C.

perature effect was found in the range 400–1000°C. No published information was found on the decomposition species of MATB and DATB. Land et al. [19] investigated the thermal decomposition of TATB by thermogravimetric modulated beam mass spectrometry. They found that the major decomposition products formed were the lower molecular mass species: H_2O, HCN, CO, NO, HNCO, CO_2 and C_2N_2, although significant amounts of high-molecular-mass species in the range *m/z* 210–256 were also formed and assigned to furoxan and furazan derivatives. Apparently these compounds were not stable at the pyrolysis temperature used, which was 340°C. TATB seems to form significant amounts of cyanogen (*m/z* 26 in Table 3). We could not find any correlation between the low-molecular-mass decomposition products and the number of NH_2 groups in the molecule.

Fig. 9 shows suggested decomposition pathways of MATB. The main fragmentation pathway is through cleavage of two C–C bonds. In some instances this occurs while keeping part or all of the NH_2 and NO_2 groups still bonded to the C atoms. A typical example is the fragment ion in MATB at *m/z* 98, due to $C_3NH_2NO_2$. These fragments then decompose further, producing the low-molecular-mass species CNO_2, HCO_2, CO, NO and CN.

3.3. Tetryl

Tetryl is both a nitroaromatic and a nitramine compound. Fig. 10 shows the Py–GC–MS RIC of tetryl at 1000°C and Fig. 11 shows an example of a mass spectrum of tetryl at that same temperature. Decomposition species from tetryl have not been previously reported.

Table 4 shows the molecular ions obtained in the Py–GC–MS of tetryl in the range 400–1000°C. No major temperature effect was found in this range. Table 4 shows the fragments also found in RDX, HMX, MATB, DATB and TATB. Fig. 12 shows suggested thermal decomposition pathways of tetryl. Most of the fragments are produced through cleavage of the bond between the carbon atom of the nitroaromatic ring and the nitraminic nitrogen atom.

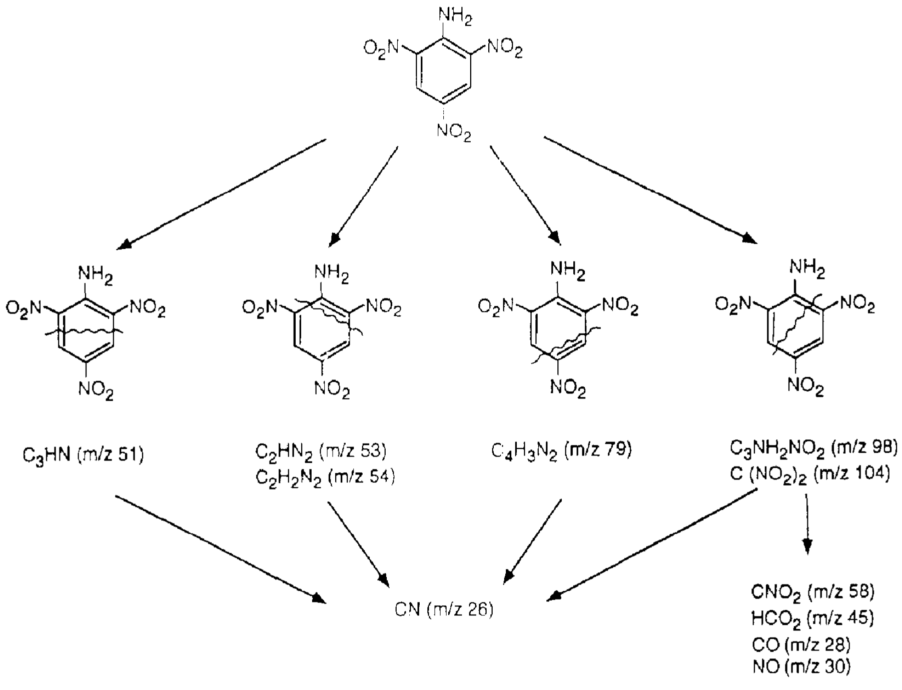

Fig. 9. Thermal fragmentation pathways of MATB.

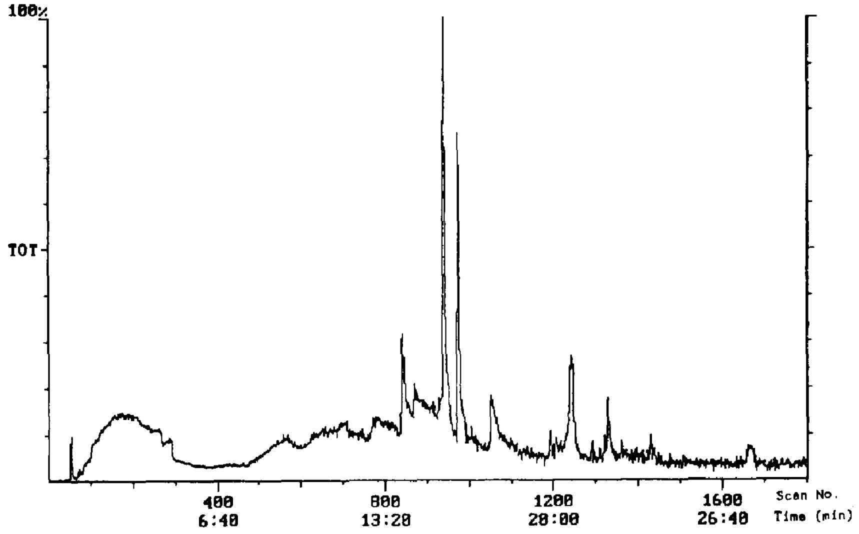

Fig. 10. Py-GC-MS: reconstructed ion chromatogram of tetryl at 1000°C.

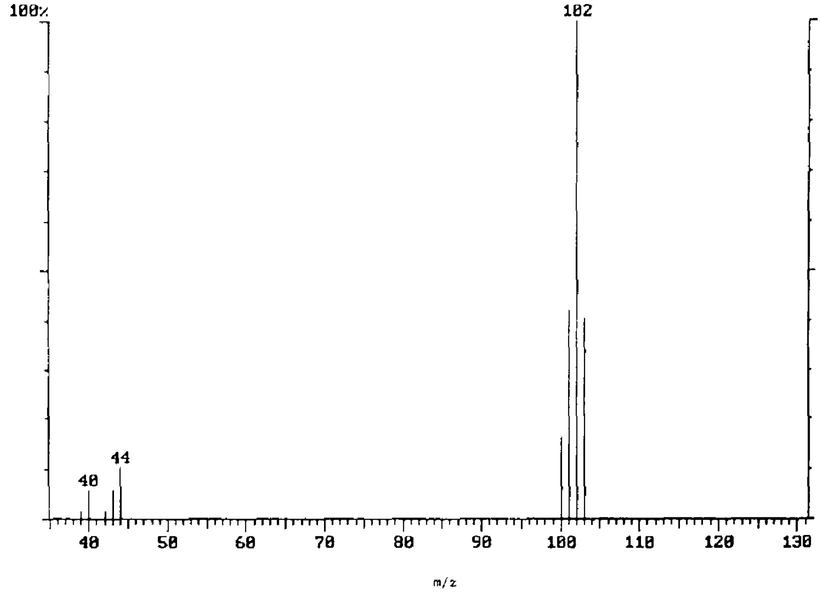

Fig. 11. Py-GC-MS: mass spectrum of a decomposition product of tetryl from pyrolysis at 1000°C.

Table 4
Molecular ions obtained in the Py–GC–MS of tetryl

m/z	Suggested formula	Also found in				
		RDX	HMX	MATB	DATB	TATB
28	CH_2N^+ or CO^+	+	+	+	+	+
29	CH_3N^+	–	–	–	–	–
30	NO^+	+	+	+	+	+
43	$CHNO^+$	+	+	–	+	+
44	CH_2NO^+	+	+	–	+	+
45	CH_3NO^+	–	+	+	–	–
52	$C_3H_2N^+$	–	–	–	–	–
53	$C_3H_3N^+$ or $C_2HN_2^+$	+	+	+	–	–
57	$C_2H_3NO^+$ or CHN_2O^+	+	–	–	–	+
58	$CH_2N_2O^+$ or CNO_2^+	+	+	+	+	+
59	$CH_3N_2O^+$ or $CHNO_2^+$	+	+	–	+	+
60	$CH_2NO_2^+$	–	+	–	–	–
65	$C_3NH_2^+$	–	–	–	–	–
77	$CH_5N_2O_2^+$ or $C_4NH_2^+$	–	–	–	–	–
103	$C_2H_3N_2O_3^+$ or $CHN_3O_3^+$	–	–	–	–	–

+ = Obtained; – = not obtained.

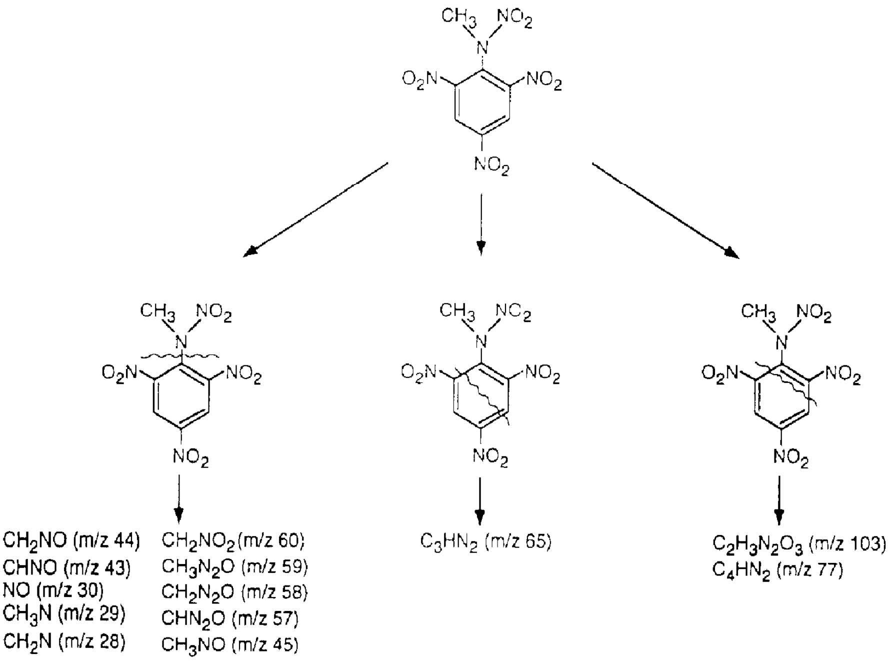

Fig. 12. Thermal fragmentation pathways of tetryl.

This fragmentation produces the species having low molecular mass up to m/z 60. Higher molecular mass fragments are formed through cleavage of two C–C bonds of the nitroaromatic ring.

4. Conclusions

Important chemical species were observed in the pyrolysis of several explosives in the temperature range of 400–1000°C, consisting of mostly low-molecular-mass species. These products resulted mainly from the cleavage of the C–C ring structure in the nitroaromatic compounds and the C–N ring structure in the nitramines. As expected, many of the higher molecular mass species, formed under thermal decomposition conditions at much lower temperatures, were not found. In several explosives, toxic species were formed during pyrolysis.

Acknowledgement

We thank Dr. Dean D. Fetterolf of FBI Laboratory in Quantico, VA, USA, for the loan of the pyrolyser.

References

[1] R.N. Rogers, *Anal. Chem.*, 39 (1967) 730.
[2] N.A. Newlon and J.L. Booker, *J. Forensic Sci.*, 24 (1979) 87.
[3] L. Huwei and F. Ruonong, *Thermochim. Acta*, 138 (1989) 167.
[4] A.P. Snyder, J.H. Kremer, S.A. Liebman, M.A. Schroeder and R.A. Fifer, *Org. Mass Spectrom.*, 24 (1989) 15.
[5] A.P. Snyder, S.A. Liebman, M.A. Schroeder and R.A. Fifer, *Org. Mass Spectrom.*, 25 (1990) 61.
[6] A.P. Snyder, S.A. Liebman, S. Bulusu, M.A. Schroeder and R.A. Fifer, *Org. Mass Spectrum.*, 26 (1991) 1109.
[7] B. Suryanarayana, R.J. Graybush and J.R. Autera, *Chem. Ind. (London)* 52 (1967) 2177.
[8] J.N. Bradley, A.K. Butler, W.D. Capey and J.R. Gilbert, *J. Chem. Soc., Faraday Trans. 1*, 73 (1977) 1789.
[9] M. Farber and R.D. Srivastava, *Chem. Phys. Lett.*, 64 (1979) 307.
[10] M. Farber and R.D. Srivastava, *Chem. Phys. Lett.*, 80 (1981) 345.
[11] R. Behrens, Jr., *J. Phys. Chem.*, 94 (1990) 6706.
[12] R. Behrens, Jr., and S. Bulusu, *J. Phys. Chem.*, 95 (1991) 5838.
[13] R. Behrens, Jr., and S. Bulusu, *J. Phys. Chem.*, 96 (1992) 8877.
[14] R. Behrens, Jr., and S. Bulusu, *J. Phys. Chem.*, 96 (1992) 8891.
[15] R. Behrens, Jr., and S. Bulusu, presented at the *29th JANNAF Combustion Meeting, NASA Langley Research Center, Hampton, VA, October 1992.*
[16] J. Yinon and S. Zitrin, *Modern Methods and Applications in Analysis of Explosives*, Wiley, Chichester, 1993.
[17] R.F.C. Brown, *Pyrolytic Methods in Organic Chemistry*, Academic Press, New York, 1980, Ch. 2.
[18] W.J. Irwin, in J.D. Winefordner (Editor), *Treatise on Analytical Chemistry. Part I. Thermal Methods*, Vol. 13, by Wiley, New York, 1993.
[19] T.A. Land, W.J. Siekhaus, M.F. Foltz and R. Behrens, Jr., in *Proceedings of the 10th International Detonation Symposium, Office of Naval Research, Arlington, VA, 1993*, in press.